



TEXT AND REFERENCES ACCOMPANYING NEVADA BUREAU OF MINES AND GEOLOGY OPEN-FILE REPORT 2025-06

# Geologic Map of Spanish Springs Peak Quadrangle, Washoe County, Nevada

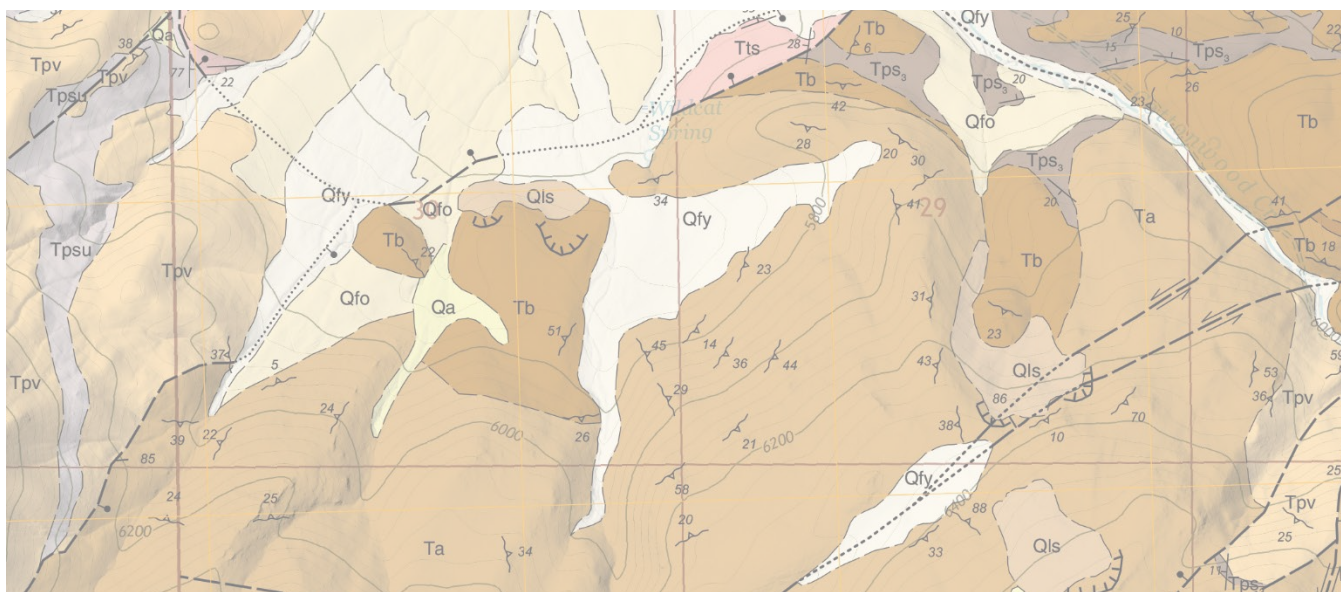
by

William Junkin<sup>1,2</sup> and Seth Dee<sup>2</sup>

<sup>1</sup>*Department of Environmental Engineering and Earth Sciences, Clemson University*

<sup>2</sup>*Nevada Bureau of Mines and Geology, University of Nevada, Reno*

2025



© Copyright 2025 The University of Nevada, Reno. All Rights Reserved.

**Suggested citation:**

Junkin, W., and Dee, S., 2025, Geologic map of the Spanish Springs Peak quadrangle, Washoe County, Nevada: Nevada Bureau of Mines and Geology Open-File Report 2025-06, scale 1:24,000, 21 p.

*NBMG open-file reports have not undergone formal peer review. This geologic map was funded in part by the USGS National Cooperative Geologic Mapping Program under the STATEMAP award number G22AC00578, 2022.*

## ABSTRACT

Mapping within the Spanish Springs Peak quadrangle provides insight into Oligocene–Miocene depositional processes, the geometry of the southern end of the Quaternary-active Warm Springs Valley fault system, and the distribution of Oligocene ash-flow tuffs that serve as key structural markers for Walker Lane tectonic deformation. Rock units in the map area include Mesozoic granitic plutonic, metasedimentary, and metavolcanic rocks; multiple Oligocene ash-flow tuff units; intercalated Miocene basalt/basaltic-andesite flows, clastic deposits including coarse tuffaceous breccia and megabreccia, and a dacitic tuff; Miocene mafic and felsic intrusions; and unconsolidated Quaternary sediments. A prominent deposit of the Oligocene tuff of Painted Hills several hundred meters thick with no exposed base crops out in the map area. This and other newly mapped Oligocene ash-flow tuffs support the previously proposed approximate location of an east-west trending Oligocene paleovalley several hundred meters deep that extends through the north half of the quadrangle. Basalt to basaltic-andesite lava flows intercalated with laterally discontinuous, coarse breccia and megabreccia deposits overlie the ash-flow tuffs. The megabreccia deposits, which attain a maximum thickness of approximately 200 m, contain predominantly tuff clasts, including clasts as large as 10s of meters in diameter, and share similarities to other megabreccia deposits in northwest Nevada interpreted as originating from landslides or “dam-burst” type floods. New geochronologic data from Miocene lavas and intercalated tuffs provide age controls and constraints on the timing of volcanism and tectonic extension in the map area. A newly dated dacitic tuff near the base of the sedimentary basin deposits in southern Warm Springs Valley indicates that extension and basin opening began prior to ~10.8 Ma, synchronous with widespread volcanism in the area. Several previously unmapped fault strands observed in newly available LiDAR data displace late Pleistocene alluvial fan surfaces and trend parallel to strands of the Warm Springs Valley fault system previously mapped to the north.

## DESCRIPTION OF MAP UNITS

### Quaternary Deposits

**Qfy Young alluvial-fan deposits (Holocene)** Young alluvial deposits in active and recently abandoned alluvial fans and washes. Grain size grades from boulder-gravels in mountain channels and adjacent to range fronts, to pebble-cobble gravels and sand in range-front proximal fans and axial drainages. Qfy grades into and includes young

pediment veneers of colluvium. Clasts are commonly subangular to subrounded. Coarse deposits are typically clast supported with a basinward increase in matrix support; weakly stratified throughout. Generally characterized by a distributary depositional pattern, but unit also commonly includes channelized alluvium (Qa). Deposited by debris flows and flood events onto active, or recently active, alluvial fans and in active washes or channels incised into Qfi, Qfo, and bedrock. Surfaces in coarser-grained deposits commonly have rough bar-and-swale morphology. Soil development ranges from absent to weak A/Bw/C profiles, where cambic (Bw) horizons are weakly developed and reach as much as 20 cm thick. Clasts are predominantly basalt, basaltic-andesite, tuff, granitic rocks, and (locally) hornblende basaltic-andesite derived from adjacent mountains. Deposits are up to 3 m thick.

**Qa Alluvium (Holocene)** Coarse- to fine-grained alluvial deposits in active axial washes; typically sandy with pebble- to cobble-sized gravel. Fresh bar-and-channel morphology with minimal soil development. Exposed thickness of the unit is typically 1–4 m. Clasts are generally subrounded to subangular. Age-correlative, and commonly lumped, with Qfy. Deposits typically 0.5 m to more than 2 m thick.

**Qfi Intermediate-aged alluvial-fan deposits (late Pleistocene)** Coarse-grained alluvial deposits in inactive alluvial fans and terraces. Grain size at range fronts comprised largely of boulder-gravels, grading finer basinward to pebble-cobble gravels and gravely sand. Clasts are commonly subangular to subrounded. Coarse deposits are typically clast supported with a basinward increase in matrix support; weakly stratified throughout. Surfaces are generally smooth, planar, moderately dissected, and topographically higher than inset Qfy fans. Soil profiles typically have eolian sand and silt caps (A or Av) with varying thicknesses, iron-stained horizons (Bw) up to 50 cm thick, and moderately developed, structured argillic horizons (Bt) up to 40 cm thick. Deposits are up to 4 m thick.

**Qfo Older alluvial-fan deposits (middle Pleistocene)** Coarse-grained alluvial deposits in inactive or relict alluvial fans and terraces. Grain size at range fronts with non-granitic bedrock exposed typically comprised largely of boulder-gravels, grading basinward to pebble-cobble gravels. Clasts are commonly subangular to subrounded. Surfaces are generally smoothed, broadly rounded, and well dissected. Qfo alluvial-fan surfaces are typically topographically higher than adjacent, inset Qfi surfaces. Commonly capped by a lag of varnished basalt cobbles and

boulders, granite cobbles, and tuff pebbles. Soil profiles typically have eolian sand and silt caps (A or Av) with varying thicknesses, iron-stained horizons (Bw) up to 1 m thick, and well-developed structured argillic (Bt) horizons up to 70 cm thick. Deposits are as much as 4 m thick.

**Qls Landslide deposits (Holocene to late Pleistocene)**

Coarse, unconsolidated debris composed of clasts of basalt, basaltic-andesite, and tuff eroded from steep flanks of adjacent mountain slopes. Surfaces commonly have hummocky topography. Blocks up to 4+ m in diameter. Deposits reach at least 25 m in thickness.

**QTf Oldest alluvial-fan deposits (early Pleistocene to Pliocene?)** Coarse-grained alluvial deposits in relict alluvial fans and high-standing alluvial deposits. Comprised largely of sandy pebble- to cobble-sized, subangular to subrounded clasts. Commonly capped by a lag of varnished basalt cobbles and boulders, granite cobbles, and tuff pebbles. Exposed thickness of the unit rarely exceeds 4 m.

**QTb Unconsolidated boulder deposits (early Pleistocene to Pliocene?)** Unconsolidated boulder-rich deposit with subrounded clasts typically 0.5–1.5 m in diameter with occasional clasts up to 3 m in diameter. The boulder deposit is exposed in one location along the western edge of the map area, where it overlies units Tb and Ta. Clasts are predominantly basalt. Exposed thickness of the unit is 3–4 m.

## Miocene Volcanic and Sedimentary Rocks

**Tts Sandstone and siltstone, tuffaceous (Pliocene to Miocene)** Predominantly whitish-tan to whitish-gray lithic sandstone and siltstone, with lesser conglomerate, pebbly sandstone, mudstone, finely laminated shale, and thinly bedded ash-fall tuff. Sandstone deposits are well bedded and commonly contain tabular and trough cross-bedding, ripple marks, and fining-upward cycles. The sandstone in Tts is commonly poorly sorted and immature, with subangular grains. Deposits vary locally in composition, ranging from predominantly tuffaceous at most locations in the quadrangle, to increasingly granitic where proximate to Kgr outcrops. Clasts in pebbly sandstone and conglomerate commonly include rhyolitic ash-flow tuff, basalt and basaltic-andesite, granitic rocks, and metasedimentary rocks. Tts is locally intercalated with mafic lava flows and volcanic breccia (Tba) as well as at least one primary tuff (Tt). The Tts unit is the principal basin fill sedimentary unit exposed in southern Warm Springs Valley. Estimated thickness is 500 m in the north of the map area and thins southeastward to where it onlaps underlying

Miocene volcanic rocks at the southern edge of Warm Springs Valley.

A sample of hornblende from an ash bed intercalated in deposits equivalent to unit Tts just to the north in the adjacent Moses Rock quadrangle yielded an  $^{40}\text{Ar}/^{39}\text{Ar}$  plateau age of  $8.86 \pm 0.30$  Ma (sample # H99-48; table 1; Garside et al., 2003).

**Tba Basalt and basaltic-andesite (late Miocene)** Basalt and basaltic-andesite flows interbedded in Tts sedimentary layers. Flows exhibit variable vesicularity and are moderately to abundantly porphyritic, with a typical phenocryst assemblage of 5–15% very fine (1 mm) olivine (commonly iddingsitized to reddish-brown blocky aggregates), 5–10% 1–2 mm plagioclase feldspar, and minor clinopyroxene. Individual flows are typically 1–2 m thick, with multiple flows forming stacks as thin as a few meters to as thick as approximately 50 m.

A sample from a basalt flow in Warm Springs Valley yielded an  $^{40}\text{Ar}/^{39}\text{Ar}$  whole rock isochron age of  $9.24 \pm 1.32$  Ma (sample # H99-47; table 1; Garside et al., 2003).

**Ta Andesite, basalt, and basaltic-andesite (late Miocene)** Dark gray to tan-weathering mafic to intermediate lava flows and volcanic breccia. Rock types include abundantly porphyritic to glomeroporphyritic andesite with coarse phenocrysts and glomerocrysts of clinopyroxene (<1%), orthopyroxene (~1%), opacitic hornblende (<1%), and plagioclase feldspar (~20%) in a hypocrySTALLINE groundmass of weakly to unaligned plagioclase feldspar laths; aphyric to sparsely porphyritic basaltic-andesite with sparse opacitic hornblende phenocrysts (<1%) in a hypocrySTALLINE groundmass with moderately to weakly aligned plagioclase feldspar laths; and fine-grained porphyritic basalt with microphenocrysts of plagioclase feldspar (10–15%) and skeletal, iddingsitized olivine (~1%) in a holocrystalline groundmass of strongly aligned plagioclase feldspar laths and intergranular pyroxene granules. Alteration of groundmass and of mafic phenocrysts is common throughout the unit: groundmass glass is almost universally altered or devitrified, olivine is commonly partially or completely iddingsitized, and hornblende phenocrysts are typically completely altered to pseudomorphic cryptocrystalline masses of opaque minerals, with primary hornblende only rarely preserved in the interiors of coarse phenocrysts.

The Miocene volcanic sequence in the quadrangle exhibits variable stratigraphic relationships, with unit Ta in depositional contact with the underlying units Tb, Tps<sub>3</sub>, and



Tpv at different locations. Similarity in outcrop appearance between Ta, Tb, and Tpv results in uncertainty with respect to the areal extent of these three units, particularly along the southern border of the quadrangle. Unit Ta is distinguished from the underlying Tb and Tpv lavas based on a relatively high percentage of plagioclase phenocrysts and presence of hornblende phenocrysts. Unit Ta may share the same stratigraphic position as the dacite of Pond Peak, mapped in the adjacent Olinghouse quadrangle to the east (Garside and Bonham, 2006), although the relationship between these two units remains unresolved. Maximum exposed thickness of the unit ranges from 300–700 m, although faulting complicates thickness estimates.

A sample of plagioclase from a Ta lava flow yielded an  $^{40}\text{Ar}/^{39}\text{Ar}$  weighted mean age of  $9.58 \pm 0.35$  Ma (sample # SP23SD-350; table 1)

**Tt Unnamed dacitic tuff (late Miocene)** White to very pale gray dacitic tuff. Lowest exposed 1–1.5 m of outcrop is a pale gray, poorly sorted, weakly bedded, normally graded lapilli tuff consisting of a fine-grained ashy matrix, volcanic lithic fragments, and flattened white pumices up to 4 cm in length but typically 1–2 cm in length. Densely packed pumices at the base of the lapilli tuff have aspect ratios as high as ~5:1. The 1–1.5 m of lapilli tuff is overlain along a sharp contact by a sequence of three layers, each one cm in thickness, of normally graded, well sorted, medium-grained volcanic crystals and lithic fragments possibly representing a surge deposit and suggesting the underlying lapilli tuff may represent a pyroclastic density current. The possible surge deposit is overlain by 4–5 m of white to very pale gray, weakly stratified tuff with a fine-grained, well sorted ashy matrix and medium-grained lithics and volcanic crystals likely representing a minimally reworked ash-fall tuff. The ash-fall tuff grades upwards into 4–5 m of well bedded, white to very pale gray, likely reworked tuffaceous material. Unit Tts is well exposed in a gully east of, and adjacent to, Cottonwood Creek, where it is overlain by siltstones and sandstones of unit Tts and a lava flow of unit Tba. Total deposit thickness is approximately 12 m.

A sample of plagioclase from the ash-fall tuff portion of the unit yielded an isochron  $^{40}\text{Ar}/^{39}\text{Ar}$  age of  $10.786 \pm 0.037$  Ma (sample # SP23SD-131; table 1).

**Ts Sedimentary rocks, tuffaceous (late Miocene)** Sedimentary rocks intercalated throughout map unit Tb. Includes pebble conglomerate, sandstone, and siltstone. Commonly poorly exposed and mapped based on float of pebbles of ash-flow tuff and chips of finer-grained material intercalated in Tb lavas. Where outcrops are exposed Ts is

pale gray to pale yellow, thinly bedded and commonly tuffaceous. Sandstone and pebble conglomerate beds are typically moderately well-sorted sandstone with local cross-bedding. Rounded clasts are composed predominantly of intermediate to silicic tuffaceous material with varying lesser proportions of granitic and mafic volcanic material. Deposits range in thickness from less than 1 m (smaller than a mappable unit at this scale) to 50 m thick.

**Tb Basalt (late Miocene)** Dark-gray- to dark-brown-weathering, dark-gray olivine basalt flows with lesser basaltic-andesite flows. Massive to locally platy jointed and crudely columnar jointed, commonly vesicular. Phenocrysts (commonly <5%) of olivine ( $\leq 1$  mm), partly to completely altered to iddingsite with lesser plagioclase, and, rarely, orthopyroxene. Individual flows  $\leq 10$  m; total thickness unknown, but probably several hundred meters. Tb lava flows cap much of the Curnow Range west of southern Warm Springs Valley. The lava flow sequence dips westward and thickens to the east. Unit Tb is correlative with the Lousetown Formation basaltic rocks mapped in the adjacent Griffith Canyon quadrangle (Garside et al., 2010) and discussed in Bonham and Papke (1969).

A whole rock sample from a unit Tb basaltic-andesite lava flow collected on the slopes just northwest of Spanish Springs Peak yielded an  $^{40}\text{Ar}/^{39}\text{Ar}$  plateau age of  $11.26 \pm 0.120$  Ma (sample # GC218b; Garside et al., 2003; table 1). A whole rock matrix sample from a basalt flow ca. 100 m east of the top of unit Tb yielded an isochron  $^{40}\text{Ar}/^{39}\text{Ar}$  age of  $10.743 \pm 0.034$  Ma (sample # 22WJ-1169; table 1). A sample of plagioclase from a basalt flow near the southeastern corner of the quadrangle yielded a whole rock matrix  $^{40}\text{Ar}/^{39}\text{Ar}$  age of  $10.699 \pm 0.022$  Ma (sample SP23SD-368; table 1).

### **Middle Miocene Pyramid Sequence**

**Tpsu Pyramid sequence sedimentary rocks, undivided (middle Miocene?)** Sedimentary rocks intercalated throughout Miocene volcanic rocks. Includes breccia, conglomerate, sandstone, siltstone, and megabreccia. Commonly occurs as eroded, chaotically strewn boulders, cobbles, and/or pebbles of ash-flow tuff, with finer-grained material very poorly exposed in steep walls of drainages and roadcuts and in saddles eroded between peaks of more resistant Tpv rocks. Tuffaceous, very pale gray to pale yellow sandstone and pebble conglomerate is poorly exposed but clearly comprises a significant fraction of the overall unit. Sandstone deposits generally range from massive and poorly sorted pebbly sandstone with subangular to

subrounded tuff pebbles, to well-bedded and moderately well-sorted sandstone with both planar- and cross-bedding.

Deposits are composed predominantly of intermediate to silicic tuffaceous material with varying lesser proportions of granitic and mafic volcanic material. In addition, breccia, conglomerate, and sandstone composed of predominantly basaltic and basaltic-andesite material occur within Wilcox Canyon and on the northeastern lower slopes of Spanish Springs Peak.

Deposits range in thickness from less than 1 m (unmapped) to several hundred meters (Tps<sub>2mb</sub>).

**Tps<sub>2-3</sub> Pyramid sequence sedimentary rocks, subunits 2–3 (middle Miocene)** Each numbered subunit corresponds to discontinuous outcrops of sedimentary rocks, predominantly tuffaceous, interpreted to be a correlated map-scale group of deposits occurring within Tpv at the same stratigraphic interval across the quadrangle. Lithologic descriptions for each subunit are the same as Tpsu except where separately mapped as Tps<sub>2mb</sub> and Tps<sub>3mb</sub>. Tps<sub>3</sub> appears to be the most laterally continuous of the subunits and commonly occurs at or just below the contact separating Tpv from overlying volcanic units (Ta, Tb).

At several locations near the southeast edge of the quadrangle, a dacitic tuff <1 m in thickness, ranging from moderately reworked to strongly welded, occurs at the top of Tps<sub>3</sub> sedimentary deposits, just below the contact with overlying mafic volcanic rocks (Ta, Tpv). A sample of plagioclase from one such welded tuff outcrop yielded an <sup>40</sup>Ar/<sup>39</sup>Ar weighted mean age of 11.441 ± 0.032 Ma (sample # SP23SD-099; table 1).

**Tps<sub>3mb</sub> Pyramid sequence sedimentary rocks, subunit 3 (megabreccia facies) (middle Miocene)** Reddish-orange, dark brown, and brownish-yellow, clast-supported, tuffaceous breccia and megabreccia composed primarily of angular to subrounded clasts of undivided ash-flow tuff commonly up to 1 m in diameter but as large as 10 m in diameter. Tuff clasts exhibit a large variety of textures, pumice contents, and phenocryst assemblages, as well as variable silicification. Matrix is poorly exposed and consists of still finer, variably silicified breccia. In addition to several map-scale bodies of Tps<sub>3mb</sub>, smaller, unmapped, similar tuffaceous megabreccia deposits occur as lenses throughout Tps<sub>3</sub> in the northern half of the quadrangle. Thickness is as much as 15 m.

**Tps<sub>2mb</sub> Pyramid sequence sedimentary rocks, subunit 2 (megabreccia facies) (middle Miocene)**

Light brown, reddish-orange, and pale greenish-gray megabreccia, breccia, pebble conglomerate, and sandstone. Appears as eroded, chaotically strewn, isolated cobbles and boulders or piles of the same with sparse, poorly exposed outcrops. Clasts consist of ash-flow tuff, granitic rock, mafic volcanic rocks, and locally quartzite, with tuff and granitic boulders as large as 4 m. Locally, clasts vary from predominantly ash-flow tuff (resembles Tps<sub>3mb</sub>) to predominantly granitic rock. Well-sorted, planar- and cross-bedded sandstone and pebble conglomerate clearly comprise a significant proportion of the unit but are poorly exposed. Maximum thickness is 320 m, although thickness varies considerably across the map area.

**Tps<sub>1</sub> Pyramid sequence sedimentary rocks, subunit 1 (middle Miocene)**

Pale pinkish-gray volcanic breccia, very poorly exposed. Outcrops are weakly stratified and consist of multiple several-m-thick layers of poorly sorted volcanic breccia with separate breccia flows defined by subtle compositional differences in clasts. No fine-grained layers separate breccia flows. Breccia is clast supported with an oxidized reddish matrix. Clasts are exclusively volcanic, consist of a variety of colors and compositions, and are typically less than 15 cm in diameter. Appears to grade upwards into Tps<sub>2mb</sub>, although upper contact is very poorly exposed. Maximum thickness is at least 100 m with no exposed base.

**Tpv Pyramid sequence lavas (middle Miocene)**

Basalt and basaltic-andesite flows and subordinate pyroclastic and volcanoclastic deposits.

Flows are typically 1–30 m thick and range from coarsely and densely porphyritic, to finely and sparsely porphyritic, to aphyric. Phenocrysts include tabular plagioclase up to 1 cm long, equant plagioclase typically 1–2 mm in diameter, pyroxene typically 1–2 mm but as large as 5 mm in diameter, and olivine typically 0.5–2 mm in diameter and commonly altered to iddingsite. Locally includes glomerocrysts of plagioclase and pyroxene up to 1 cm in diameter. Matrix typically consists of plagioclase, olivine, pyroxene, opaque minerals, and variably altered volcanic glass. The upper parts of flows are commonly vesicular and foliated, with considerable variation observed in measured flow foliations. Local vertical columnar jointing is also common, as is autobrecciation at the base of flows.

Individual flows overlie and/or interfinger with sedimentary deposits and commonly terminate abruptly, with map patterns suggesting steep flow margins and coeval sedimentation in steep-walled paleovalleys developed in an actively incising landscape. Tpv volcanic rocks are intercalated with map-scale deposits of tuffaceous sedimentary rocks (Tpsu, Tps<sub>1</sub>, Tps<sub>2</sub>, Tps<sub>2mb</sub>, Tps<sub>3</sub>, Tps<sub>3mb</sub>, Tps<sub>4</sub>) and smaller, unmapped deposits of both tuffaceous sedimentary rocks and sedimentary rocks of mafic to intermediate composition. The latter include matrix-supported volcanic breccia with a brown sandy matrix, and planar-bedded dark brownish-red silty sandstone. Poorly exposed, sub map-scale mafic pyroclastic deposits are also intercalated with lava flows and consist of densely packed mafic lapilli and volcanic bombs up to 40 cm in diameter in a dark brown to brownish-yellow matrix of altered ash.

In mountains on the east flank of the Warm Springs Valley, Tpv includes rocks previously mapped as the Pyramid sequence (Bonham and Papke, 1969; Garside and Bonham, 2006). This study mapped Tpv in the ranges on either side of the Warm Springs Valley as equivalent and undivided, on the basis of the virtually identical tuffaceous sedimentary stratigraphy intercalated within the Tpv sections throughout the map area.

Including intercalated sedimentary units (Tpsu, Tps<sub>1-4</sub>), Tpv reaches a maximum thickness of approximately 1000 m.

Ages determined for the Pyramid sequence and regionally similar rocks range from 18 Ma (see summary in Henry et al., 2004) to 11 Ma (Sadowski and Faulds, 2016). In the Olinghouse quadrangle immediately east of the Spanish Springs Peak quadrangle, a whole rock plateau <sup>40</sup>Ar/<sup>39</sup>Ar age of 13.10 ± 0.04 Ma was acquired from a lava at the base of the Pyramid sequence (sample # OG285; table 1; Garside and Bonham, 2006). These ages are consistent with sample SP23SD-099 (<sup>40</sup>Ar/<sup>39</sup>Ar 11.441 ± 0.032 Ma) collected from a tuff in unit Tps<sub>3</sub> that conformably overlies the Pyramid sequence lavas that are exposed in the map area.

## Oligocene Ash-Flow Tuffs

**Tph Tuff of Painted Hills (late Oligocene)** Brownish-gray to light gray to white, nonwelded to moderately welded, resistant, porphyritic, ash-flow tuff. Forms ledges and cliffs.

Commonly overlain by 0.5 m or thicker reworked tuffaceous sedimentary deposits with mostly Tph clasts including megabreccia, breccia, conglomerate, and pebbly sandstone. May correlate with the tuff of Elevenmile Canyon of the Stillwater Range (John, 1995), which is petrographically similar and has an indistinguishable age. Maximum thickness of Tph in the map area is at least 320 m with no exposed base. A sample of sanidine yielded an <sup>40</sup>Ar/<sup>39</sup>Ar age of 25.083 ± 0.018 Ma (sample # 22WJ-0083; table 1).

**Tnh Nine Hill Tuff (late Oligocene)** A sample of sanidine from Tnh exposed in the Dogskin Mountain quadrangle approximately 20 kilometers to the northwest yielded an <sup>40</sup>Ar/<sup>39</sup>Ar age of 25.25 ± 0.06 Ma (sample # MC-10; table 1; Henry et al., 2004).

Tnh subcrop occurs at one location in the northeast corner of the Spanish Springs Peak quadrangle.

The following unit description is from Delwhiche (2007): Tnh is a widely distributed ash-flow tuff found throughout central and western Nevada and north-eastern California (Deino, 1985). Yellowish-orange or reddish-brown, sparsely porphyritic and moderately to nonwelded lower zone and moderately porphyritic and densely welded upper zone ash-flow tuff. Lower Tnh contains 3–6% phenocrysts, including sanidine (3–6%, 0.5–1 mm wide and 3–4 mm long), plagioclase (0–1%, 1 mm wide and 3mm long), rare ‘smokey’ quartz (<0.5%, 1–2 mm long), rare biotite (<0.5% and <1 mm long), and rare anorthoclase. Upper Tnh contains 10–15% phenocrysts of sanidine (4–8%, 0.5–1 mm wide and 3–4 mm long), plagioclase (<1–2%, 0.5–1 mm wide and 2–3 mm long), rare ‘smokey’ quartz (<0.5% and 1–2 mm long), rare biotite (<0.5% and <1 mm long), and rare anorthoclase. The Nine Hill Tuff is distinguished from other ash-flow tuffs by traces of hornblende, an abundance of sanidine (up to 8%), a paucity of biotite, the presence of three feldspars in thin-section, rare ‘smokey’ quartz, and high aspect ratios of compaction foliations (e.g. up to 16:1). Lower Tnh contains <5% pumice, and upper Tnh contains ~5–10% pumice. Pumice cavities and small lithophysae may contain visible products from vapor phase recrystallization that include fine-grained (<0.5 mm long) spherulites of quartz and feldspar. The tuff also contains rare lithic fragments of porphyritic felsic volcanic rocks. Tnh has irregular vertical cooling columns that overprint compaction foliations. Unlike most ash-flow tuffs, Tnh weathers into blocky and tabular clasts. In the Pah Rah Range, Tnh overlies a disconformable surface carved into the tuff of Dogskin Mountain, laterally changes thickness abruptly from 0–100 m, and is commonly missing between the tuff of Dogskin

Mountain and the tuff of Chimney Spring. Tnh is either highly channelized or eroded prior to deposition of younger ash-flow tuffs.

**Tmc Tuff of Mine Canyon (early Oligocene)** Reddish-orange, pale-red, or reddish-brown porphyritic, moderately welded ash-flow tuff. Tmc contains 10–15% phenocrysts of plagioclase (oligoclase 4–10%, 0.5–2 mm wide and 2–3 mm long), sanidine (2–5%, 0.5–1 mm wide and 3–4 mm long), and biotite (1–2%, 1–2.5 mm long). Relative to the tuff of Dogskin Mountain, Tmc is slightly less porphyritic and contains less, but larger average biotite phenocrysts and more sanidine. Compaction foliations exhibit aspect ratios of ~4.5:1. Relative to Twc, Tmc has more biotite and less sanidine. The tuff grades into a pinkish-white upper nonwelded zone that contains more biotite. Description from Delwiche (2007). A sample of sanidine from the adjacent Moses Rock quadrangle to the north yielded an  $^{40}\text{Ar}/^{39}\text{Ar}$  age of  $29.98 \pm 0.05$  Ma (sample # F03-340; table 1; Delwiche, 2007).

A Tmc outcrop with a maximum thickness of 40–60 m crops out at one location in the northeast corner of the Spanish Springs Peak quadrangle, where it overlies Kgr along a nonconformable contact and overlies Twc along a depositional or faulted contact. A sample of sanidine from this location yielded an  $^{40}\text{Ar}/^{39}\text{Ar}$  age of  $30.115 \pm 0.040$  Ma (sample # 22WJ-0662; table 1).

**Twc Tuff of Cove Spring (early Oligocene)** A sample of sanidine from the adjacent Moses Rock quadrangle to the north yielded an  $^{40}\text{Ar}/^{39}\text{Ar}$  age of  $30.08 \pm 0.06$  Ma (sample #F03-343; table 1; Delwiche, 2007).

Twc crops out at three locations in the northeast corner of the Spanish Springs Peak quadrangle, where it nonconformably overlies Kgr and ranges in thickness from 0–70 m. Three samples of sanidine yielded overlapping  $^{40}\text{Ar}/^{39}\text{Ar}$  ages of  $30.300 \pm 0.037$ ,  $30.219 \pm 0.038$  Ma, and  $30.341 \pm 0.021$  Ma, respectively (sample #'s 22WJ-0668, 22WJ-0740, 22WJ-0885; table 1).

Description from Delwiche (2007): Red to reddish-brown sparsely porphyritic, moderately to densely welded lower zone and white sparsely porphyritic nonwelded upper zone. Twc contains 8–12% phenocrysts of sanidine (7–9%, 0.5–2 mm wide and 2–3 mm long), plagioclase (1%, 0.5–2 mm wide and 2–3 mm long), biotite (<0.5–1%, 0.5–1.5 mm long), and traces of quartz (<1 mm). The tuff consists of a moderately to densely welded lower zone that grades into a nonwelded upper zone containing more biotite. Twc contains ~5% pumice and commonly exhibits a compaction

foliation with aspect ratios ~5:1. Reddish-brown opal that commonly fills compacted pumice cavities may have formed from post-eruption hydrous transport and deposition of quartz. The lower welded zone is massive and grades upward into the nonwelded white zone. Columnar joints overprint compaction foliations. Exposed surfaces commonly exhibit ‘nubbly’ weathering. Higher concentrations of sanidine (7 to 9% compared to 4 to 6%) and generally smaller biotite (<1.5 mm compared to 2.5 mm) help distinguish this tuff from the lower tuff of Axehandle Canyon. Lesser amounts of plagioclase (1% compared to 4–10%) and biotite (1% compared to 2%) distinguish Twc from Tmc.

**Tsu Tuff of Sutcliffe (early Oligocene)** A sample of sanidine from the Dogskin Mountain quadrangle approximately 20 kilometers to the northwest yielded an  $^{40}\text{Ar}/^{39}\text{Ar}$  age of  $30.41 \pm 0.07$  Ma (sample # H02-41; table 1; Henry et al., 2004).

Tsu crops out at one location in the northwest corner of the Spanish Springs Peak quadrangle, where its thickness is uncertain. A sample of sanidine from this location yielded an  $^{40}\text{Ar}/^{39}\text{Ar}$  age of  $30.558 \pm 0.025$  Ma (sample # 22WJ-1032; table 1).

Description from Delwiche (2007): Purplish-gray or pinkish-gray moderately to densely welded porphyritic ash-flow tuff. The tuff consists of a nonwelded basal zone, moderately to densely welded middle, and weakly welded upper zone that is rarely preserved. The lower nonwelded zone is purple moderately porphyritic, containing ~15% phenocrysts of plagioclase (oligoclase 8%, ~1–2 mm wide and 3–4 mm long), sanidine (7%, ~2–3 mm wide and 3–4 mm long), and biotite (~0.5%, 1–2 mm long). Felsic porphyritic, volcanic lithic fragments are ~1% of the lower zone. The middle zone consists of 20–30% phenocrysts of plagioclase (10–20%, 0.5–2.5 mm wide and 3–4 mm long), sanidine (4–10%, <0.5–2.5 mm wide and 3–4 mm long), and biotite (1–3%, <0.5–2 mm long). Phenocryst content decreases up section. Pumice content ranges from 1–5% and compaction foliations exhibit aspect ratios of ~4:1. Lithics (including porphyritic felsic volcanic fragments) form up to 1–4% of the middle zone. Tsu may have vertical meter-scale columnar joints that overprint compaction foliations. A sparse pumice content, larger average phenocrysts, presence of felsic lithic fragments, and lower aspect ratios distinguish Tsu from the tuff of Axehandle Canyon.

**Ttu Ash-flow tuffs, undivided (Oligocene)** Undivided ash-flow tuffs. Outcrops display a variety of colors, textures, and phenocryst assemblages and are all exposed as fault-bounded slivers in contact with Mesozoic basement rocks,



or as strata deposited on Mesozoic basement rocks. Over 150 m of undivided ash-flow tuffs are exposed in the northwest corner of the map area.

## Tertiary(?) Intrusive Rocks

**Tai Intrusive basalt, basaltic-andesite, and andesite (late Miocene)** Dikes, sills, and plugs of material compositionally equivalent to Ta intruding Tpv and Tps<sub>3</sub> in the southeast corner of the quadrangle. Given the possible interfingering relationship between Tpv and Ta, and the difficulty of distinguishing Tpv from Ta in outcrop, some rocks mapped as Tai may be volcanic flows of Ta interlayered in Tpv.

**Thi Hornblende basaltic-andesite irregular intrusions (Tertiary?)** Undivided, irregular intrusions of porphyritic basaltic-andesite with moderately abundant to abundant phenocrystic hornblende (5–10%) and variably abundant phenocrystic plagioclase (0–5%). Hornblende phenocrysts commonly exhibit opaque (opacitic) reaction rims, form elongate bladed crystals and lesser blocky prisms typically 1–2 mm in length but rarely up to 1 cm, and commonly exhibit simple twinning. Plagioclase phenocrysts form blocky prisms commonly less than 1–2 mm. Groundmass is fine-grained, greenish-yellow to dark greenish-gray, and variably altered to clay minerals. Contains sparse xenocrysts of intergrown blocky plagioclase feldspar crystals and fine, needle-shaped hornblende crystals. In the northwest corner of the map area, map-scale bodies form irregular contacts with Kgr and Tps<sub>2mb</sub>, and with Ttu within fault-bounded blocks; smaller unmapped bodies separate Ttu and Tsu from Kgr in the northwest corner of the map area, and Tnh from Kgr in the northeast corner of the map area. Near the east edge of the map area in the Wilcox Canyon area, an unmapped concordant, tabular body of Thi intercalated within Tpsu strata just below the contact with overlying Tpv lava flows may represent a sill of Thi or a locally restricted extrusive equivalent. The largest intrusions occur in the northwest corner of the map area and may reach at least 150 m in thickness, although faulting and the irregularity of intrusive contacts complicate thickness estimates.

**Tri Rhyolitic dike (Tertiary?)** A porphyritic rhyolite dike crops out within Mzms near the contact with Kgr. The dike is several meters thick and extends horizontally approximately 180 m. The rhyolite is composed of ~30% phenocrysts in a microsilica groundmass. Phenocrysts include potassium feldspar (15%) with skeletal texture; rounded, embayed quartz (10%); biotite (1–3%);

plagioclase feldspar (1–2%); fine-grained aggregates of feldspar, quartz, and biotite (1–2%); and accessory titanite.

## Cretaceous Granitic Rocks

**Kgr, Kgr<sub>1</sub>, Kgr<sub>2</sub> Granitic rocks, undivided (quartz monzodiorite, granodiorite, diorite) (Cretaceous)** Pale tan to dark gray, undivided granitic rocks, including diorite, quartz monzodiorite, and granodiorite.

Quartz monzodiorite is generally fine- to coarse-grained and equigranular, although primary foliation occurs locally in the northeast corner of map area. Quartz monzodiorite consists of plagioclase, quartz, alkali feldspar, biotite, hornblende, and pyroxene. Locally cut by felsic intrusions including aplitic veins and dikes and by hornblende basaltic-andesite intrusions (Thi). Locally contains diorite and gabbroic diorite enclaves.

Granodiorite is commonly medium-grained and consists of plagioclase, quartz, alkali feldspar, biotite, and hornblende with accessory sphene and magnetite. Locally cut by hornblende basaltic-andesite intrusions (Thi) and aplitic dikes, and locally contains mafic enclaves. In the northeast corner of the map area, Kgr<sub>1</sub> hosts a raft or pendant of Mesozoic metamorphosed volcanic and/or sedimentary rocks mapped separately (Mzms). U-Pb crystallization ages were determined for zircon grains separated from quartz monzodiorite samples collected at two locations.

A sample collected in Curnow Canyon in the Griffith Canyon quadrangle, at a location ca. 120 m west of the western boundary of the Spanish Springs Peak quadrangle near its northwestern corner, yielded a zircon <sup>238</sup>U/<sup>206</sup>Pb weighted mean age of 94.18 ± 0.73 Ma (sample # 22WJ-1179; fig. 1a; table 2). A sample collected from the center of the large area of Kgr<sub>1</sub> cropping out in the northeast corner of the Spanish Springs Peak quadrangle yielded a significantly older zircon <sup>238</sup>U/<sup>206</sup>Pb weighted mean age of 105.38 ± 0.75 Ma (sample # 22WJ-1180; fig. 1b; table 2).

## Jurassic(?) Metamorphic Rocks

**Mzms Metamorphosed sedimentary and volcanic rocks, undivided (Jurassic?)** Dark gray to pale gray metamorphosed volcanic and sedimentary rocks. Overwhelmingly fine- to coarse-grained amphibolite with lesser quartzite, metasilstone, and slate. Occurs in the northeast corner of the map area as one unbroken pendant or raft hosted by quartz monzodiorite and intruded by aplitic and rhyolitic veins and dikes (e.g., Tri). Amphibolite exhibits a metamorphic foliation that dips steeply to

moderately to the north. Crops out across a 0.7 km<sup>2</sup> area; the geometry of the unit at depth is uncertain.

## ACKNOWLEDGMENTS

Research supported by the USGS National Cooperative Geologic Mapping Program under STATEMAP award number G22AC00578, 2022. The views and conclusions contained in this document are those of the authors and should not be interpreted as necessarily representing the official policies, either expressed or implied, of the U.S. Government.

## REFERENCES

- Bonham, H.F., and Papke, K.G., 1969, Geology and mineral deposits of Washoe and Storey counties, Nevada: Nevada Bureau of Mines and Geology Bulletin 70, 139 p.
- Deino, A.L., 1985, Stratigraphy, chemistry, K-Ar dating, and paleomagnetism of the Nine Hill Tuff, California-Nevada—Miocene/Oligocene ash-flow tuffs of Seven Lakes Mountain, California-Nevada—improved calibration methods and error estimates for potassium-40-argon-40 dating of young rocks: Berkeley, University of California, Ph.D. dissertation, 457 p.
- Delwiche, B.M., 2007, Oligocene paleotopography and structural evolution of the Pah Rah Range, western Nevada—implications for constraining slip on the right-lateral Warm Springs Valley fault in the northern Walker Lane: University of Nevada, M.S. thesis, Reno, 138 p.
- Garside, L.J., and Bonham, H.F., Jr., 2006, Geologic map of the Olinghouse quadrangle, Nevada: Nevada Bureau of Mines and Geology Open-File Report 2003-29, 1:24,000.
- Garside, L.J., Castor, S.B., dePolo, C.M., and Davis, D.A., 2003, Geologic map of the Fraser Flat quadrangle and the west half of the Moses Rock quadrangle, Washoe County, Nevada: Nevada Bureau of Mines and Geology Map 146.
- Garside, L.J., Nials, F.L., and Ramelli, A.R., 2010, Preliminary geologic map of the Griffith Canyon quadrangle, Washoe County, Nevada: Nevada Bureau of Mines and Geology Open-File Report 2010-2, 1:24,000, 7 p.
- Gehrels, G.E., Valencia, V.A., and Ruiz, J., 2008, Enhanced precision, accuracy, efficiency, and spatial resolution of U-Pb ages by laser ablation–multicollector–inductively coupled plasma–mass spectrometry: *Geochemistry, Geophysics, Geosystems*, v. 9, no. 3, 13 p.
- Henry, C.D., Castor, S.B., Starkel, W.A., Ellis, B.S., Wolff, J.A., Laravie, J.A., McIntosh, W.C., and Heizler, M.T., 2017, Geology and evolution of the McDermitt caldera, northern Nevada and southeastern Oregon, western USA: *Geosphere*, v. 13, no. 4, p. 1066–1112, doi:10.1130/GES01454.1.
- Henry, C.D., Faulds, J.E., dePolo, C.M., and Davis, D.A., 2004, Geologic map of the Dogskin Mountain quadrangle, Nevada: Nevada Bureau of Mines and Geology Map 148.
- John, D.A., 1995, Tilted middle Tertiary ash-flow calderas and subadjacent granitic plutons, southern Stillwater Range, Nevada—cross sections of an Oligocene igneous center: *Geological Society of America Bulletin*, v. 107, p. 180–200.
- Ludwig, K., 2008, Isoplot version 4.15—a geochronological toolkit for Microsoft Excel: Berkeley Geochronology Center Special Publication, 76 p.
- Middlemost, E.A.K., 1994, Naming materials in the magma/igneous rock system: *Earth-Science Reviews*, v. 37, no. 1–4, p. 215–224.
- Sadowski, A.J., and Faulds, J.E., 2016, Preliminary geologic map of the Truckee Range, Black Warrior geothermal area, Washoe and Churchill counties, Nevada: Nevada Bureau of Mines and Geology Open-File Report 2016-7, 1:24,000.
- Stacey, J.S., and Kramers, J.D., 1975, Approximation of terrestrial lead isotope evolution by a two-stage model: *Earth and Planetary Science Letters*, v. 26, p. 207–221.
- Steiger, R.H., and Jäger, E., 1977, Subcommission on geochronology—convention on the use of decay constants in geo- and cosmochemistry: *Earth and Planetary Science Letters*, v. 36, p. 359–362, doi: 10.1016/0012-821X(77)90060-7.
- Taylor, J.R., 1982, An introduction to error analysis—the study of uncertainties in physical measurements: Mill Valley, California, University Science Books, 270 p.

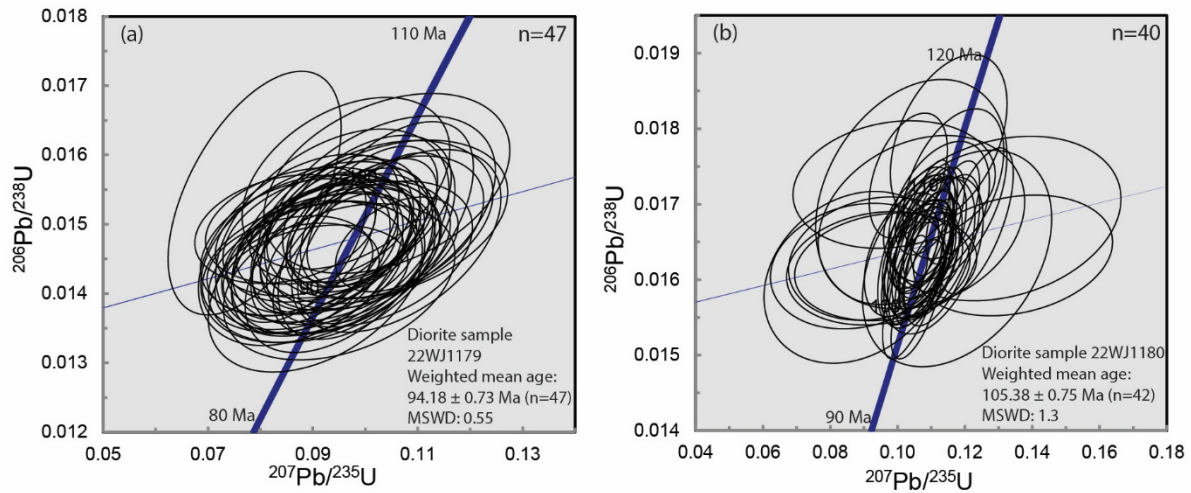


**Figure 1.** U-Pb concordia diagrams showing results of analyses of zircon grains from undivided granitic rocks (Kgr). Data point error ellipses are 2σ. Results are summarized in table 2.

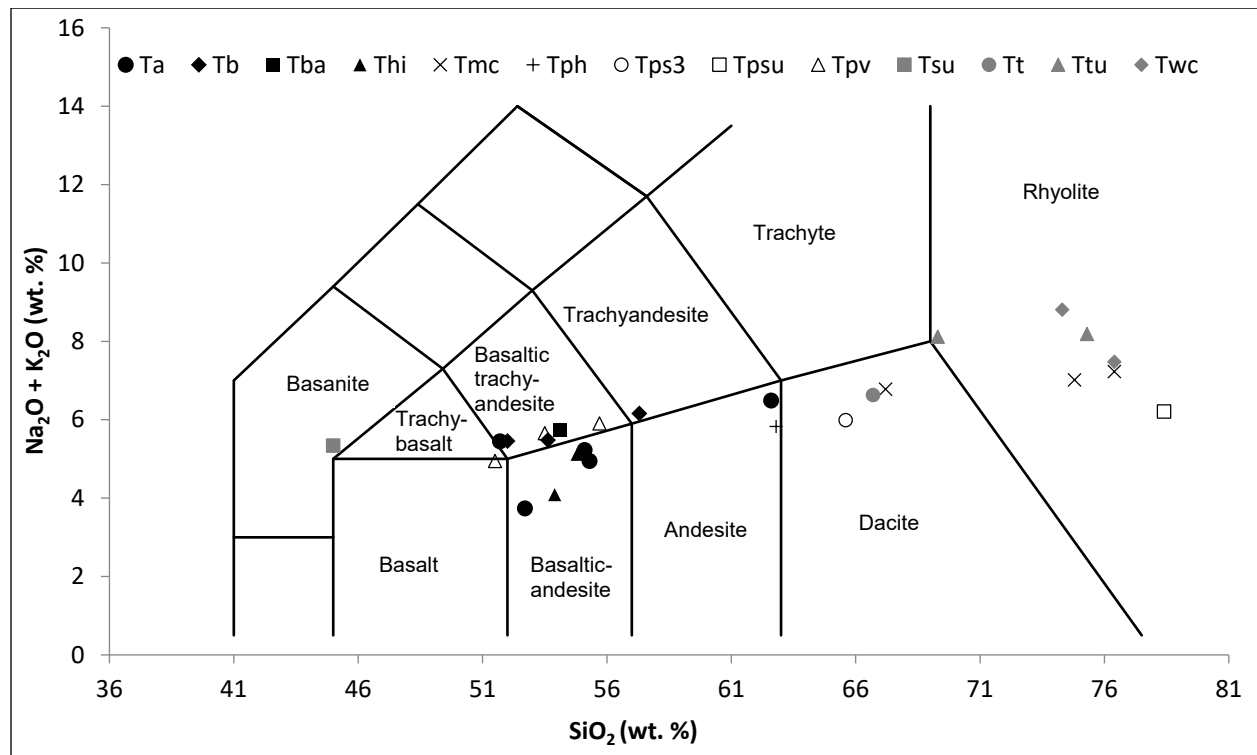


**Figure 1.** New geochemical data for volcanic rocks analyzed in the Spanish Springs Peak quadrangle. Data are provided in table 3 and are plotted in the total alkali versus silica (TAS) diagram of Middlemost (1994). One sample was collected and analyzed by Garside et al. (2003). Sample 22WJ-1032, collected from an outcrop of the tuff of Sutcliffe (Tsu), plotted in the "basanite" field; we do not consider this composition representative of the unit.

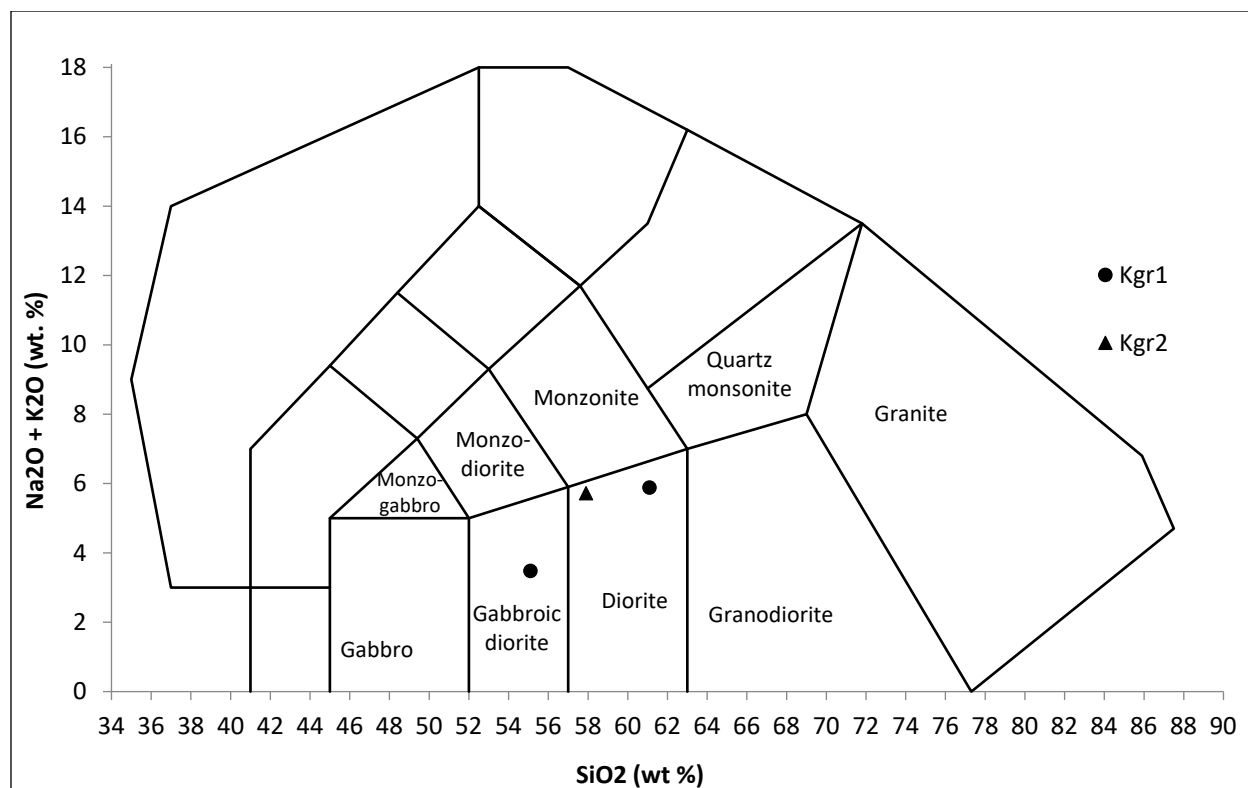


**Figure 3.** New geochemical data for plutonic rocks analyzed in the Spanish Springs Peak quadrangle. Data in table 3 and are plotted in a total alkali versus silica (TAS) diagram of Middlemost (1994).



**Table 1.  $^{40}\text{Ar}/^{39}\text{Ar}$  dates, Spanish Springs Peak area.**

Sample #	Material	Age method	Age (Ma)	$\pm 2s$	K/Ca	$\pm 1s$	n**	Map symbol	Map unit	Latitude	Longitude	Reference
H99-47*	whole rock	isochron	9.24	1.32	-	-	100	Tba	Basalt and basaltic-andesite	39° 41.920'	-119° 33.660'	Garside et al., 2003
H99-48*	hornblende	plateau	8.86	0.30	-	-	82.1	-	Ash bed in a correlative deposit with unit Tts in this study	39° 45.260'	-119° 34.290'	Garside et al., 2003
GC-218b*	whole rock	plateau	11.26	0.12	-	-	50.7	Tb	Basalt	39° 40.570'	-119° 36.420'	Garside et al., 2003
OG-285	whole rock	plateau	13.10	0.04	-	-	26.7	-	Pyramid sequence lavas	39° 43.71'	-119° 27.17'	Garside and Bonham, 2006
22WJ-0083	sanidine	weighted mean	25.083	0.018	55.9	4.3	22	Tph	Tuff of Painted Hills	39° 41.630'	-119° 31.333'	this study
MC-10	sanidine	weighted mean	25.25	0.06	9.1	2.4	15	Tnh	Nine Hill Tuff	39° 53.930'	-119° 41.180'	Henry et al., 2004
F03-340	sanidine	weighted mean	29.98	0.05	52.5	120.0	11	-	Tuff of Mine Canyon	39° 46.377'	-119° 33.881'	Delwiche, 2007
22WJ-0662	sanidine	weighted mean	30.115	0.040	28.5	3.6	18	Tmc	Tuff of Mine Canyon	39° 44.442'	-119° 31.955'	this study
F03-343	sanidine	weighted mean	30.08	0.06	32.8	15.4	10	Twc	Tuff of Cove Spring	39° 45.856'	-119° 33.533'	Delwiche, 2007
22WJ-0668	sanidine	weighted mean	30.300	0.037	32.4	4.0	20	Twc	Tuff of Cove Spring	39° 44.446'	-119° 31.944'	this study
22WJ-0740	sanidine	weighted mean	30.219	0.038	33.9	1.8	25	Twc	Tuff of Cove Spring	39° 43.947'	-119° 30.535'	this study
22WJ-0885	sanidine	weighted mean	30.341	0.021	31.6	7.0	24	Twc	Tuff of Cove Spring	39° 44.251'	-119° 31.448'	this study
H02-41	sanidine	weighted mean	30.41	0.07	32.4	5.2	15	Tsu	Tuff of Sutcliffe	39° 57.546'	-119° 51.506'	Henry et al., 2004
22WJ-1032	sanidine	weighted mean	30.558	0.025	33.1	4.1	12	Tsu	Tuff of Sutcliffe	39° 44.301'	-119° 37.087'	this study
SP23SD-099	plagioclase	weighted mean	11.441	0.032	0.08	0.009	5	Tps <sub>3</sub>	Pyramid sequence sedimentary rocks 3	39° 39.1394'	-119° 31.0217'	this study
SP23SD-131	plagioclase	isochron	10.786	0.037	-	-	-	Tt	Unnamed tuff	39° 41.0857'	-119° 33.2783'	this study
SP23SD-350	plagioclase	weighted mean	9.58	0.35	0.01	0.002	7	Ta	Andesite, basalt, and basaltic-andesite	39° 38.647'	-119° 32.3524'	this study
SP23SD-368	matrix	isochron	10.699	0.022	-	-	-	Tb	Basalt	39° 37.9436'	-119° 31.79'	this study
22WJ-1169	matrix	isochron	10.743	0.034	-	-	-	Tb	Basalt	39° 43.267'	-119° 32.8909'	this study

\*recalculated relative to FC-2 Fish Canyon Tuff interlaboratory standard at 28.201 Ma. See Garside et al. (2003) for full methods.

\*\*n=% of total  $^{39}\text{Ar}$  in plateau (H99-48, H99-47, GC218b), milligrams analyzed (OG-218), or number of single grains analyzed (all other samples)

Minerals were separated from crushed, sieved samples by standard magnetic and density techniques; feldspars were leached with dilute HF to remove matrix and handpicked. All analyses at New Mexico Geochronological Research Laboratory, New Mexico Institute of Mining and Technology. Analytical methods in Henry et al. (2017). Mean age is weighted mean age of Taylor (1982). Mean age error is weighted error of the mean (Taylor, 1982), multiplied by the root of the MSWD where MSWD>1, and also incorporates uncertainty in J factors and irradiation correction uncertainties. Isotopic abundances after Steiger and Jäger (1977). Ages calculated relative to FC-2 Fish Canyon Tuff sanidine interlaboratory standard at 28.201 Ma and total 40K decay constant of  $5.463\text{e-}10$  /a.

**Table 2. U-Pb dates, Spanish Springs Peak area.**

Sample #	<sup>238</sup> U/ <sup>206</sup> Pb			Concordia			n*	Map symbol	Map unit	Latitude	Longitude	Reference
	weighted mean age (Ma)	±2s	MSWD	intercept age	±2s	MSWD						
22WJ-1179	94.18	0.73	0.55	94.66	0.91	0.54	47/47	Kgr <sub>2</sub>	Granitic rocks, undivided	39° 43.526'	-119° 37.589'	this study
22WJ-1180	105.38	0.75	1.3	105.38	0.65	1.4	42/42**	Kgr <sub>1</sub>	Granitic rocks, undivided	39° 44.781'	-119° 31.108'	this study

\*n=number of analyses used in age calculations/number of single grains analyzed

\*\*Two analyses excluded because they fell outside of the dominant age population

Laser ablation multicollector inductively coupled plasma mass spectrometry (LA-MC-ICPMS) analyses conducted at the Arizona LaserChron Center. Analyses conducted by LA-MC-ICPMS, as described by Gehrels et al. (2008). U concentration and U/Th ratios are calibrated relative to Sri Lanka zircon standard and are accurate to ~20%. Common Pb correction is from measured <sup>204</sup>Pb with common Pb composition interpreted from Stacey and Kramers (1975). Common Pb composition assigned uncertainties of 1.5 for <sup>206</sup>Pb/<sup>204</sup>Pb, 0.3 for <sup>207</sup>Pb/<sup>204</sup>Pb, and 2.0 for <sup>208</sup>Pb/<sup>204</sup>Pb. U/Pb and <sup>206</sup>Pb/<sup>207</sup>Pb fractionation is calibrated relative to fragments of a large Sri Lanka zircon of 563.5 ± 3.2 Ma (2-sigma). U decay constants and composition as follows: <sup>235</sup>U = 9.8485 x 10<sup>-10</sup>, <sup>238</sup>U = 1.55125 x 10<sup>-10</sup>, <sup>238</sup>U/<sup>235</sup>U = 137.88. Weighted mean ages, concordia intercept ages, concordia plots, and 2 sigma uncertainties determined with Isoplot (Ludwig, 2008).

Table 3. Whole-rock geochemical data, Spanish Springs Peak quadrangle.

Sample	22WJ-0095	22WJ-0127	22WJ-0189	22WJ-0631	22WJ-0662	22WJ-0668	22WJ-0674	22WJ-0740	22WJ-0916
Latitude	39.698924	39.698496	39.742783	39.743217	39.740705	39.740778	39.745845	39.732455	39.742724
Longitude	-119.5278	-119.5089	-119.6225	-119.547871	-119.5326	-119.5324	-119.5522	-119.5089	-119.5376
Map Unit	Tph	Thi	Thi	Mzms	Tmc	Twc	Kgr <sub>1</sub>	Twc	Tmc
Lithology	Andesitic tuff	Basaltic-andesite intrusion	Basaltic-andesite intrusion	Granodioritic gneiss	Dacitic tuff	Rhyolitic tuff	Gabbroic diorite	Rhyolitic tuff	Rhyolitic tuff
<i>Major elements (wt. %)</i>									
SiO <sub>2</sub>	62.8	53.9	54.8	64.8	67.2	74.3	55.1	76.4	74.8
Al <sub>2</sub> O <sub>3</sub>	15.75	18.55	17.30	16.85	14.75	14.15	17.50	13.15	12.05
FeO	-	-	-	-	-	-	-	-	-
Fe <sub>2</sub> O <sub>3</sub>	4.00	7.36	7.63	4.00	2.24	2.15	8.11	1.07	2.15
CaO	4.63	7.50	6.79	6.06	1.83	0.28	3.86	0.34	0.51
MgO	1.94	4.29	4.02	1.64	0.42	0.16	8.47	0.19	0.27
Na <sub>2</sub> O	3.37	3.18	3.42	5.31	2.52	1.47	1.92	2.44	2.56
K <sub>2</sub> O	2.46	0.91	1.70	1.02	4.26	7.34	1.56	5.04	4.46
Cr <sub>2</sub> O <sub>3</sub>	0.002	0.005	0.007	<0.002	<0.002	<0.002	0.008	<0.002	<0.002
TiO <sub>2</sub>	0.43	0.81	0.82	0.52	0.29	0.19	0.96	0.11	0.11
MnO	0.07	0.11	0.14	0.09	0.02	0.01	0.08	0.01	0.03
P <sub>2</sub> O <sub>5</sub>	0.14	0.24	0.26	0.17	0.04	0.02	0.30	0.03	0.01
SrO	0.05	0.11	0.08	0.05	0.10	0.01	0.05	<0.01	0.01
BaO	0.10	0.08	0.08	0.04	0.33	0.06	0.04	0.04	0.01
LOI	4.13	2.91	2.76	0.48	7.09	1.78	2.54	1.47	3.74
Total	99.87	99.96	99.81	101.03	101.09	101.92	100.50	100.29	100.71
<i>Trace elements (ppm)</i>									
Ba	-	-	-	-	-	-	-	-	-
Ce	-	-	-	-	-	-	-	-	-

<b>Cr</b>	-	-	-	-	-	-	-	-	-
<b>Cs</b>	-	-	-	-	-	-	-	-	-
<b>Cu</b>	-	-	-	-	-	-	-	-	-
<b>Dy</b>	-	-	-	-	-	-	-	-	-
<b>Er</b>	-	-	-	-	-	-	-	-	-
<b>Eu</b>	-	-	-	-	-	-	-	-	-
<b>Ga</b>	-	-	-	-	-	-	-	-	-
<b>Gd</b>	-	-	-	-	-	-	-	-	-
<b>Hf</b>	-	-	-	-	-	-	-	-	-
<b>Ho</b>	-	-	-	-	-	-	-	-	-
<b>La</b>	-	-	-	-	-	-	-	-	-
<b>Lu</b>	-	-	-	-	-	-	-	-	-
<b>Nb</b>	-	-	-	-	-	-	-	-	-
<b>Nd</b>	-	-	-	-	-	-	-	-	-
<b>Ni</b>	-	-	-	-	-	-	-	-	-
<b>Pb</b>	-	-	-	-	-	-	-	-	-
<b>Pr</b>	-	-	-	-	-	-	-	-	-
<b>Rb</b>	-	-	-	-	-	-	-	-	-
<b>Sc</b>	-	-	-	-	-	-	-	-	-
<b>Sm</b>	-	-	-	-	-	-	-	-	-
<b>Sn</b>	-	-	-	-	-	-	-	-	-
<b>Sr</b>	-	-	-	-	-	-	-	-	-
<b>Ta</b>	-	-	-	-	-	-	-	-	-
<b>Tb</b>	-	-	-	-	-	-	-	-	-
<b>Th</b>	-	-	-	-	-	-	-	-	-
<b>Tm</b>	-	-	-	-	-	-	-	-	-
<b>U</b>	-	-	-	-	-	-	-	-	-
<b>V</b>	-	-	-	-	-	-	-	-	-
<b>W</b>	-	-	-	-	-	-	-	-	-
<b>Y</b>	-	-	-	-	-	-	-	-	-
<b>Yb</b>	-	-	-	-	-	-	-	-	-



<b>Zn</b>	-	-	-	-	-	-	-	-	-
<b>Zr</b>	-	-	-	-	-	-	-	-	-

Table 3 ctd. Whole-rock geochemical data, Spanish Springs Peak quadrangle.

Sample	22WJ-1010	22WJ-1027	22WJ-1032	22WJ-1155	22WJ-1179	22WJ-1180	GC-218b*	SP23SD-099	SP23SD-131	SP23SD-350
Latitude	39.737662	39.735796	39.73836	39.741403	39.72543333	39.74635	39.67616667	39.652323	39.684761	39.644117
Longitude	-119.6205	-119.6214	-119.6181	-119.5324	-119.6264833	-119.5184667	-119.607	-119.517029	-119.554639	-119.539207
Map Unit	Ttu	Ttu	Tsu	Tmc	Kgr <sub>2</sub>	Kgr <sub>1</sub>	Tb	Tps <sub>3</sub>	Tt	Ta
Lithology	Rhyolitic tuff	Rhyolitic tuff	Basanite	Rhyolitic tuff	Diorite	Diorite	Basaltic- andesite	Dacitic tuff	Dacitic tuff	Basaltic- andesite
<i>Major elements (wt %)</i>										
SiO <sub>2</sub>	69.3	75.3	45.0	76.4	57.9	61.1	53.6	65.6	66.7	55.3
Al <sub>2</sub> O <sub>3</sub>	15.40	13.75	9.86	13.15	18.00	16.95	17.71	17.45	13.75	18.1
FeO	-	-	-	-	-	-	8.83	-	-	-
Fe <sub>2</sub> O <sub>3</sub>	2.66	2.26	2.09	1.94	6.76	5.74	-	1.75	3.84	8.77
CaO	0.98	0.32	19.80	0.40	6.03	4.85	7.49	2.15	1.17	8.11
MgO	0.44	0.26	0.35	0.14	2.63	2.09	4.51	1.28	0.55	4.89
Na <sub>2</sub> O	2.70	2.62	2.02	2.26	4.16	3.92	3.72	3.45	2.28	3.74
K <sub>2</sub> O	5.42	5.57	3.32	4.97	1.56	1.96	1.76	2.54	4.35	1.21
Cr <sub>2</sub> O <sub>3</sub>	<0.002	<0.002	<0.002	<0.002	0.002	<0.002	-	0.002	0.378	0.01
TiO <sub>2</sub>	0.33	0.14	0.21	0.11	0.66	0.50	1.59	0.36	0.22	1
MnO	0.01	0.01	0.46	0.01	0.13	0.11	0.15	0.04	0.46	0.13
P <sub>2</sub> O <sub>5</sub>	0.08	0.04	0.08	0.01	0.22	0.21	0.61	0.09	0.05	0.21
SrO	0.02	0.01	0.03	<0.01	0.08	0.06	-	0.04	0.02	0.08
BaO	0.17	0.06	0.11	0.04	0.09	0.10	-	0.14	0.13	0.09
LOI	2.30	1.24	16.10	2.00	0.57	0.63	0.06	5.02	7.51	0.21
Total	99.81	101.58	99.43	101.43	98.79	98.22	99.23	99.91	101.41	101.85
<i>Trace elements (ppm)</i>										
Ba	-	-	-	-	735	836	1040	1290	1225	847
Ce	-	-	-	-	30.4	27.2	-	46.1	47.5	30.9
Cr	-	-	-	-	14	14	65	16	31	86

<b>Cs</b>	-	-	-	-	1.68	2.13	-	3.58	4.77	0.45
<b>Cu</b>	-	-	-	-	-	-	43	-	-	-
<b>Dy</b>	-	-	-	-	3.44	2.18	-	2.36	1.92	3.84
<b>Er</b>	-	-	-	-	2.02	1.4	-	1.53	1.29	2.2
<b>Eu</b>	-	-	-	-	1.04	0.83	-	0.69	0.51	1.33
<b>Ga</b>	-	-	-	-	21	17.6	19	17.6	15	20.2
<b>Gd</b>	-	-	-	-	3.73	2.83	-	2.52	2.39	4.59
<b>Hf</b>	-	-	-	-	4.31	3.18	-	4.68	3.86	3.13
<b>Ho</b>	-	-	-	-	0.62	0.44	-	0.44	0.41	0.81
<b>La</b>	-	-	-	-	13.9	13.3	-	24.3	25.4	16.1
<b>Lu</b>	-	-	-	-	0.28	0.18	-	0.28	0.21	0.33
<b>Nb</b>	-	-	-	-	5.01	3.96	16	9.39	8.57	4.51
<b>Nd</b>	-	-	-	-	19	15.4	-	18.4	18.1	20.7
<b>Ni</b>	-	-	-	-	-	-	35	-	-	-
<b>Pb</b>	-	-	-	-	-	-	12	-	-	-
<b>Pr</b>	-	-	-	-	4.18	3.58	-	5	5.24	4.56
<b>Rb</b>	-	-	-	-	50.3	57.6	34	61.3	111.5	20.3
<b>Sc</b>	-	-	-	-	-	-	24	7	5	29.5
<b>Sm</b>	-	-	-	-	4.2	3.27	-	2.9	3.02	4.48
<b>Sn</b>	-	-	-	-	1	0.8	-	1	1.7	1
<b>Sr</b>	-	-	-	-	609	455	657	348	202	729
<b>Ta</b>	-	-	-	-	0.3	0.3	-	0.5	0.4	<0.1
<b>Tb</b>	-	-	-	-	0.54	0.38	-	0.39	0.35	0.67
<b>Th</b>	-	-	-	-	3.03	4.02	3	10.65	9.74	1.8
<b>Tm</b>	-	-	-	-	0.23	0.16	-	0.24	0.18	0.33
<b>U</b>	-	-	-	-	1.47	1.23	-	3.23	4.27	0.79
<b>V</b>	-	-	-	-	144	98	233	22	12	249
<b>W</b>	-	-	-	-	0.5	0.8	-	3.1	2.2	0.8
<b>Y</b>	-	-	-	-	16.6	12.2	25	14	13.2	22.2
<b>Yb</b>	-	-	-	-	1.58	1.39	-	1.39	1.27	1.99
<b>Zn</b>	-	-	-	-	-	-	102	-	-	-

<b>Zr</b>	-	-	-	-	168	121	237	162	133	104
-----------	---	---	---	---	-----	-----	-----	-----	-----	-----



Table 3 ctd. Whole-rock geochemical data, Spanish Springs Peak quadrangle.

Sample	SP23SD-368	22WJ-1169	23WJ-1610	23WJ-1613	23WJ-1881	22WJ-1172	22WJ-1167	22WJ-0155	SP23SD-576	23WJ-1703	22WJ-1466
Latitude	39.632393	39.721117	39.677668	39.674359	39.644399	39.702905	39.708487	39.705182	39.656204	39.647331	39.667021
Longitude	-119.529833	-119.548181	-119.50666	-119.505919	-119.578808	-119.555009	-119.620332	-119.522857	-119.621878	-119.613985	-119.592809
Map Unit	Tb	Tb	Tps <sub>3</sub>	Ta	Ta	Tba	Tb	Tpv	Ta	Ta	Tb
Lithology	Basaltic-andesite	Basaltic-andesite	Rhyolitic tuff	Andesite	Basaltic-andesite	Basaltic-andesite	Basaltic-andesite	Basalt	Basaltic-andesite	Basaltic-andesite	Andesite
<i>Major elements (wt %)</i>											
SiO <sub>2</sub>	55.7	53.5	78.4	62.6	52.7	54.1	52	51.5	51.7	55.1	57.3
Al <sub>2</sub> O <sub>3</sub>	18.55	17.6	10.1	17.2	16.45	17.6	17.3	16.75	19.1	17.55	18.45
FeO	-	-	-	-	-	-	-	-	-	-	-
Fe <sub>2</sub> O <sub>3</sub>	7.71	9.43	0.8	5.58	9.71	10.05	10.55	9.57	8.57	8.2	6.89
CaO	6.37	7.01	0.56	4.92	9.71	7.15	7.52	7.69	7.05	6.42	6.06
MgO	3.2	4.3	0.18	2.24	7.98	3.43	4.81	4.35	3.07	3.13	3.17
Na <sub>2</sub> O	4.27	4.08	2.17	4.33	2.93	4.11	3.82	3.51	4.17	3.97	4.32
K <sub>2</sub> O	1.64	1.58	4.04	2.16	0.81	1.64	1.64	1.44	1.28	1.26	1.84
Cr <sub>2</sub> O <sub>3</sub>	0.004	0.008	<0.002	<0.002	0.053	0.008	0.009	0.007	0.008	0.004	0.004
TiO <sub>2</sub>	0.94	1.3	0.11	0.65	0.83	1.3	1.52	1.48	1.1	0.89	0.88
MnO	0.12	0.14	0.02	0.08	0.15	0.17	0.15	0.15	0.13	0.12	0.12
P <sub>2</sub> O <sub>5</sub>	0.28	0.57	0.02	0.19	0.2	0.6	0.61	0.61	0.36	0.29	0.26
SrO	0.08	0.09	0.01	0.07	0.06	0.09	0.09	0.08	0.09	0.09	0.08
BaO	0.11	0.1	0.11	0.12	0.05	0.11	0.11	0.1	0.13	0.1	0.11
LOI	0.64	1.04	1.62	1.22	0.14	1.47	1.17	1.64	2.09	0.95	0.92
Total	99.61	100.75	98.14	101.36	101.77	101.83	101.3	98.88	98.85	98.07	100.4
<i>Trace elements (ppm)</i>											
Ba	973	949	968	1055	457	931	940	901	1140	831	959
Ce	41.4	60.3	24.1	36.8	21.3	63	61.7	64.9	47.8	38.4	43.3

<b>Cr</b>	40	70	<5	18	407	67	80	64	72	40	37
<b>Cs</b>	0.88	0.4	2.18	0.75	0.16	0.37	0.42	0.81	0.12	0.45	0.91
<b>Cu</b>	-	-	-	-	-	-	-	-	-	-	-
<b>Dy</b>	3.58	5.05	1.46	2.62	3.1	4.93	5.33	5.29	4.24	3.39	4.55
<b>Er</b>	2.12	2.6	0.82	1.44	1.84	2.7	2.83	2.93	2.19	1.94	2.43
<b>Eu</b>	1.31	1.94	0.25	0.99	0.84	1.99	1.76	2.05	1.54	1.25	1.32
<b>Ga</b>	20.3	20.3	9.2	18.5	15.4	18.8	19.4	19.5	21	18	20.2
<b>Gd</b>	4.48	6.3	1.44	2.86	3.12	6.62	6.67	6.55	4.98	4.25	4.85
<b>Hf</b>	4.1	4.75	2.17	3.71	1.98	4.74	4.84	5.11	4.47	3.03	4.34
<b>Ho</b>	0.78	0.97	0.31	0.52	0.62	1.05	1.07	1.08	0.8	0.68	0.91
<b>La</b>	20.1	26.8	12.2	19.6	9.1	28.1	27.9	30.2	23.7	19.8	23.5
<b>Lu</b>	0.32	0.35	0.13	0.18	0.22	0.32	0.35	0.36	0.31	0.26	0.32
<b>Nb</b>	6.15	12.05	6.47	4.96	2.88	11.65	14.65	16.85	6.89	4.54	6.5
<b>Nd</b>	23.5	34.6	8.9	16.9	13.1	33.8	33.9	34.8	25	23	24.4
<b>Ni</b>	-	-	-	-	-	-	-	-	-	-	-
<b>Pb</b>	-	-	-	-	-	-	-	-	-	-	-
<b>Pr</b>	5.44	7.74	2.78	4.47	2.7	7.77	7.69	8.02	6.18	5.27	5.82
<b>Rb</b>	28.4	21.5	83.4	42.5	11.8	24.3	30	28.2	8.9	19.8	32.2
<b>Sc</b>	22.8	21.6	5.5	15.9	39.8	20.9	22.5	24	24.5	17.2	20.1
<b>Sm</b>	5	7.08	1.95	3.68	3.66	7.14	6.99	7.04	5.61	4.65	5.14
<b>Sn</b>	1.3	1.4	0.8	0.9	0.6	1.6	1.6	1.5	1.3	0.9	1.1
<b>Sr</b>	711	794	78.6	626	554	839	801	722	827	844	711
<b>Ta</b>	0.1	0.3	0.3	0.1	0.2	0.6	0.8	0.9	0.4	0.3	0.4
<b>Tb</b>	0.61	0.86	0.25	0.47	0.49	0.88	0.89	0.95	0.73	0.61	0.7
<b>Th</b>	2	1.92	8.21	4.59	1.02	1.94	1.84	2.05	1.87	2.45	1.88
<b>Tm</b>	0.3	0.4	0.12	0.23	0.28	0.42	0.41	0.37	0.33	0.26	0.36
<b>U</b>	0.83	0.72	2.85	1.74	0.37	0.67	0.59	0.72	0.66	0.86	0.8
<b>V</b>	182	187	20	123	278	204	228	245	216	172	181
<b>W</b>	0.7	0.7	53.1	3.3	0.7	<0.5	0.7	0.5	0.8	0.8	0.5
<b>Y</b>	20.7	27.4	8.9	14.7	17.4	27.2	27.3	28.1	23.4	18.6	25.2
<b>Yb</b>	1.96	2.27	0.92	1.32	1.67	2.44	2.63	2.67	1.88	1.78	2.27

<b>Zn</b>	-	-	-	-	-	-	-	-	-	-	-
<b>Zr</b>	156	182	57	134	69	197	195	209	178	118	173

Analyses by ICP-AES (Inductively Coupled Plasma Atomic Emission Spectroscopy) (major element) and ICP-MS (trace element) at ALS Global.

\*Total Fe calculated as FeO; if originally reported as Fe<sub>2</sub>O<sub>3</sub>, recalculated as FeO. Ten major oxide values normalized to 100% after recalculation of total Fe to FeO.

Trace elements in ppm. Total is sum of 10 major oxides before normalization. LOI, loss on ignition.

Analyzed at Nevada Bureau of Mines and Geology Analytical Laboratory; analytical methods reported in Garside et al. (2003, p. 4).